



Magnetocaloric effect and refrigeration cooling power in amorphous Gd₇Ru₃ alloys

Pramod Kumar and Rachana Kumar

Citation: [AIP Advances](#) **5**, 077125 (2015); doi: 10.1063/1.4926810

View online: <http://dx.doi.org/10.1063/1.4926810>

View Table of Contents: <http://scitation.aip.org/content/aip/journal/adva/5/7?ver=pdfcov>

Published by the [AIP Publishing](#)

Articles you may be interested in

[Magneto-caloric effect of a Gd₅₀Co₅₀ amorphous alloy near the freezing point of water](#)

[AIP Advances](#) **5**, 097122 (2015); 10.1063/1.4930832

[The physical properties of Gd₃Ru: A real candidate for a practical cryogenic refrigerator](#)

[Appl. Phys. Lett.](#) **106**, 194106 (2015); 10.1063/1.4921143

[The magnetocaloric effect and critical behavior in amorphous Gd₆₀Co₄₀-xMnx alloys](#)

[J. Appl. Phys.](#) **111**, 07A922 (2012); 10.1063/1.3673860

[Large magnetocaloric effect and refrigerant capacity in Gd-Co-Ni metallic glasses](#)

[J. Appl. Phys.](#) **111**, 07A919 (2012); 10.1063/1.3673422

[Ferromagnetism and Incipient Superconductivity in a CeRu₂+7.3% GdRu₂ Alloy](#)

[J. Appl. Phys.](#) **35**, 974 (1964); 10.1063/1.1713563



Magnetocaloric effect and refrigeration cooling power in amorphous Gd₇Ru₃ alloys

Pramod Kumar^{1,a} and Rachana Kumar^{2,b}

¹Magnetic and Spintronic Laboratory, Indian Institute of Information Technology Allahabad, Allahabad 211012, India

²National Physical Laboratory, New Delhi, 110012 India

(Received 6 May 2015; accepted 30 June 2015; published online 10 July 2015)

In this paper, we report the magnetic, heat capacity and magneto-caloric effect (MCE) of amorphous Gd₇Ru₃ compound. Both, temperature dependent magnetization and heat capacity data reveals that two transitions at 58 K and 34 K. MCE has been calculated in terms of isothermal entropy change (ΔS_M) and adiabatic temperature change (ΔT_{ad}) using the heat capacity data in different fields. The maximum values of ΔS_M and ΔT_{ad} are 21 Jmol⁻¹K⁻¹ and 5 K respectively, for field change of 50 kOe whereas relative cooling power (RCP) is ~735 J/kg for the same field change. © 2015 Author(s). All article content, except where otherwise noted, is licensed under a Creative Commons Attribution 3.0 Unported License. [<http://dx.doi.org/10.1063/1.4926810>]

INTRODUCTION

Magnetocaloric refrigeration and power generation are amongst the latest solid-based refrigeration technologies used for cryogenic applications and an ideal substitute for the existing gas-based refrigeration in terms of environmentally benign, adaptability and efficiency. Also, the technology is solid state based which makes it attractive for applications such as space missions, food storage, air conditioning, gas liquefaction etc.¹⁻⁴ Magnetocaloric refrigeration is manifests as isothermal entropy change ΔS_M or adiabatic temperature change ΔT_{ad} (heating or cooling) of magnetic solids due to a varying magnetic field. The concept of magnetic refrigeration, which is based on magnetocaloric effect (MCE), has attracted a great deal of attention from a large group of researchers and has triggered an intensive search for compounds with large MCE.¹⁻⁴ Giant magnetocaloric effect (GMCE) exhibited by many intermetallic compounds render them as potential refrigerants for magnetic refrigerators.¹⁻⁴ Large value of MCE spreads over a wide temperature range is considered as one of the most important requirements of a practical magnetic refrigerant system. The compounds such as Gd₅Si₂Ge₂, MnAs, LaFe_{13-x}Si_x, MnFe(P_{1-x}As_x), RM₂ [R= rare-earth (Sm, Gd, Tb, Dy etc.) and M=transition metal (Fe, Co, Mn etc.)] and Ni₂MnGa exhibit giant magnetocaloric effect (GMCE) with first order transition (FOT) due to combining effects of field-induced magnetic transitions and/or structural transitions or Itinerant Electron Metamagnetic transition (IEM).⁵⁻¹⁰ FOT and strong magnetocrystalline coupling present several disadvantages, i.e., high hysteresis loss and hard magnetic behavior reduce the efficiency of refrigerating cooling power (RCP) [= $\Delta S_M(T) * \delta T_{FWHM}$] and structural changes promotes cracks nucleation which may cause several damages in the refrigeration materials during cycles.¹ First order transitions are sharp reducing the operating temperature range and refrigerating cooling power.

On the other hand, metallic glasses/ amorphous alloys display very unique properties, such as, (i) soft magnet with second order magnetic transition, reduced coercivity, and high permeability; (ii) tunable transition temperature by composition or annealing which is useful in application of magnetic refrigeration¹¹⁻¹⁵ taking these parameters into consideration, we study the magnetic, heat capacity and magnetocaloric effect in amorphous Gd₇Ru₃ alloys. We found that large ΔS_M and ΔT_{ad}

^aEmail Id: pkumar@iita.ac.in

^bEmail Id: rachanak@nplindia.org



spreads over 2 to above 120 K temperature range in 50 kOe field required for practical magnetic refrigerant system.

EXPERIMENTAL DETAILS

The 20-30 μm thick ribbons were prepared by melt spinning technique under argon atmosphere on rotating copper wheel with 42 ms^{-1} speed. Structural information was received by X-ray diffraction using $\text{Cu } K_{\alpha}$ radiation. Magnetization was measured using Quantum design SQUID whereas, heat capacity was measured in PPMS in the temperature ranges of 2–200 K. MCE has been calculated using M-H isotherms near transition temperature and heat capacity data in different field. Before measurement at each temperature the specimen was zero-field cooled from 60 K.

RESULTS AND DISCUSSION

Figure 1 shows the XRD patterns of Gd_7Ru_3 alloy. Obtained result shows that Gd_7Ru_3 is a fully amorphous alloy. Two very broad peaks have been observed with a maximum of 2θ values between 30° and 50° , for the first coordination shell. Another peak in the range of 55° to 75° was observed. M-T data of Gd_7Ru_3 compound collected in various applied magnetic fields both under zero field cooled (ZFC) and field cooled conditions (FCC) are shown in figure 2, whereas, inset of figure 2(a) shows the Curie-Weiss fit of the inverse (d.c.) magnetic susceptibility and inset of figure 2(b) shows the thermal hysteresis below ordering temperature. It can be seen from the figure 2(a) that M-T data shows two magnetic transitions, the first one at high temperature and the second one at roughly half of the high temperature transition. The high temperature transition seen in this compound corresponds to the onset of long range magnetic order and is denoted by T_{ord} . Low temperature transition is denoted by T_1 and has ferromagnetic nature. The M-T data collected in $H = 100 \text{ Oe}$ reveals that T_{ord} and T_1 of this compound are 58 K and 34 K respectively. Also, M-T data collected in higher fields, i.e., $H = 1 \text{ kOe}$ and 3 kOe , and 5 kOe reveals that the T_{ord} increases with increase in magnetic field. Therefore, field dependence of T_{ord} indicates that transition at T_{ord} is ferromagnetic in character. Apart from the multiple magnetic transitions, another interesting feature seen in this compound is the existence of thermomagnetic irreversibility between the ZFC and FCC magnetization data. Generally, such thermomagnetic irreversibility between the ZFC and FCC magnetization data is seen in the compounds with narrow domain wall systems.¹⁶

It can be seen from the figure 2(a) that at high temperatures, the inverse of susceptibility of this compound follows the Curie-Weiss law. The effective moment (μ_{eff}) and paramagnetic Curie

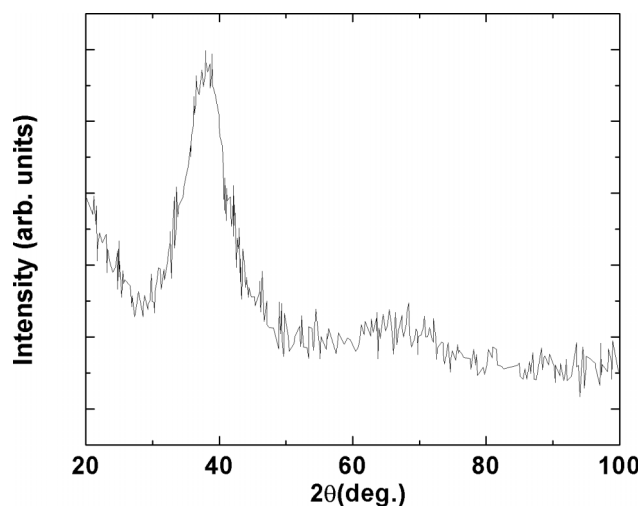


FIG. 1. XRD patterns of the amorphous Gd_7Ru_3 alloys.

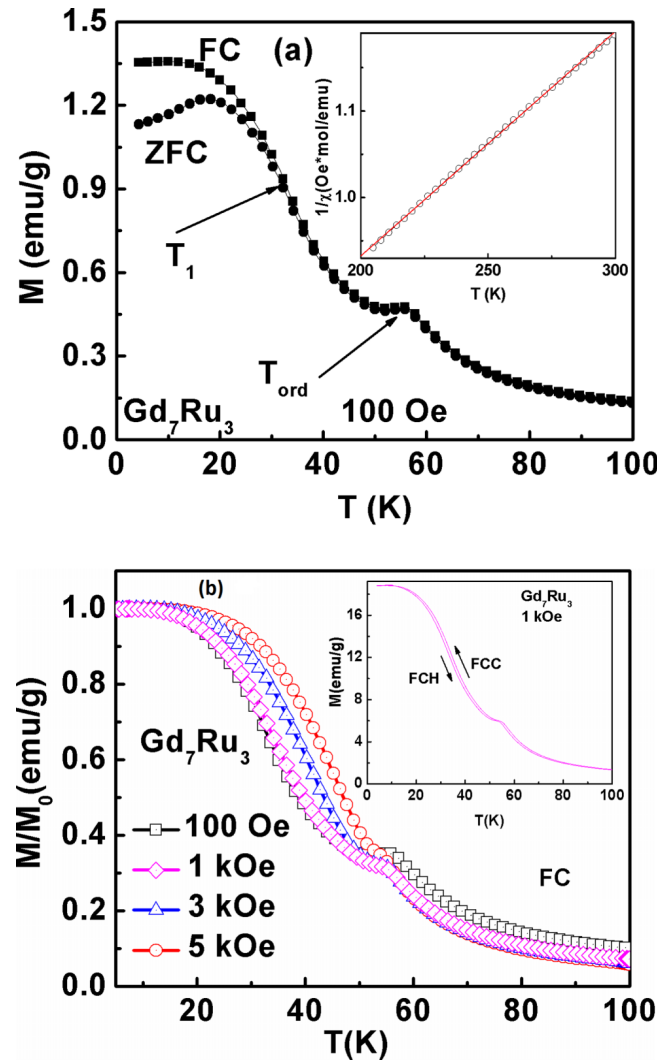


FIG. 2. (a) Temperature dependent magnetization under Zero field cooled (ZFC) and field cooled (FCC) condition at 100 Oe. Inset shows χ_{dc}^{-1} vs. T plot with Curie-Weiss fit in temperature range of 200- 300 K. Figure 2. (b) M - T in an applied field of 100 Oe, 1 kOe, 3 kOe and 5 kOe. Inset shows the extended M - T data near transition temperature for Field cooled cooling (FCC) and Field cooled heating (FCH) state at 1 kOe.

temperature (θ_p) thus obtained from the fit are $\sim 8 \mu_B$ and 159 K respectively. Although effective moments in excess of $7.94 \mu_B/\text{Gd}$ are currently interpreted in crystalline materials as being the result of conduction electron polarization, as explained by Buschow et. al., in the present material an interpretation in terms of small ferromagnetic clusters seems more appropriate.¹⁵ The distribution of nearest neighbor distances mentioned above in other extreme can lead to small regions in which the ferromagnetic coupling is stronger than the average. In such regions ferromagnetically ordered clusters may present at temperatures higher than ordering temperature where they behave as super-paramagnetic particles.

Figure 3 shows the field dependent magnetization isotherms, obtained at 5 K and up to a maximum field of 120 kOe. The M - H isotherms at different temperature in step of 5 K is shown in inset. It can be seen from the figure that saturation of magnetization is obtained above 40 kOe. At 5 K saturation magnetization is found to be $7.24 \mu_B$ in an applied field of 120 kOe. However, the gJ values corresponding to Gd^{3+} ion is $7 \mu_B$. The difference between the gJ values and the experimentally observed values, may be due to coupling between 4f electron spins proceeding to a large extent indirectly via 5d electron polarization. The 5d electronic states will split by the local

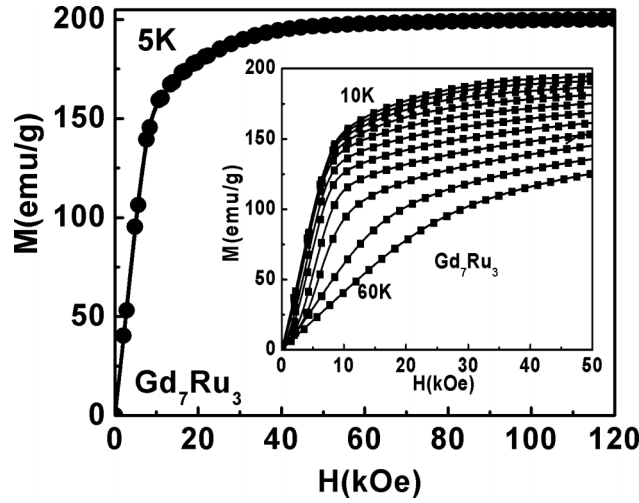


FIG. 3. M - H isotherm at 5K. Inset shows the M - H isotherms of Gd_7Ru_3 alloys near ordering temperature. Before measurements at each temperature the specimen was zero-field cooled from 100 K.

crystal field and only low lying crystal field states will be occupied by 5d electrons. It is reasonable, therefore to assume that 4f-5d coupling involves only some particular 5d orbital's and in this way leads to an anisotropic exchange interaction.

In order to further understand the nature of the magnetic state of this compound, heat capacity measurements, both under zero-field as well as in various applied fields, have been performed. The representative C vs. T plot for Gd_7Ru_3 is given in figure 4(a). It can be seen from this figure that zero-field C - T data shows two anomalies at 58 K and 34 K, which are close to the magnetic transitions seen at T_{ord} and T_1 in the M - T data of this compound (see Figure 2(a)). It may also be seen from the figure that with increase in field, the anomaly at T_{ord} gets rounded off and shift towards higher temperatures. Therefore, the C - T data also indicates that T_{ord} anomaly is ferromagnetic in character.

In order to analyze the magnetic behavior of this compound, C_{mag} (magnetic part of heat capacity) has been resolved from the zero-field heat capacity. The C_{mag} was resolved from temperature variation heat capacity data (C - T) by deduction of nonmagnetic contribution from it. The $C_{lattice}$ and C_{ele} contribution to the heat capacity was determined using equation (1). In this sample, Debye model is not a good approximation for the calculation of lattice contribution to the heat capacity. Therefore, a modified expression while taking into account the Debye and the Einstein models, as represented by the second and third terms respectively of equation (1) was used to analyze the C - T data.¹⁷⁻²²

$$C_{Lattice} + C_{ele} = \gamma T + R \left(\sum_{i=1}^{27} \frac{1}{1 - \alpha_{E_i} T} \frac{x_{E_i}^2 \exp(x_{E_i})}{[\exp(x_{E_i}) - 1]^2} + \frac{9}{1 - \alpha_D T} \left(\frac{1}{x_D} \right)^3 \int_0^{x_D} \frac{x^4 \exp(x)}{[\exp(x) - 1]^2} dx \right) \quad (1)$$

Here, γ is the coefficient of electronic specific heat, R is the universal gas constant, α_E 's and α_D 's are the anharmonicity coefficients for the optical branches and the acoustic branches, respectively; $x_{E_i} = \frac{\theta_{E_i}}{T}$ and $x_D = \frac{\theta_D}{T}$ where θ_E 's and θ_D are the Einstein and Debye temperatures, respectively. In equation (1), the first term corresponds to electronic contribution to heat capacity whereas, the second and third terms are due to the phonon contribution corresponding to the Einstein and Debye models, respectively. The coefficients α 's have been put to take care of the anharmonicity effects.²³⁻²⁵ It may further be noticed from equation (1) that in second term corresponding to the Einstein model, the summation extends from $i=1$ to 27, which is due to 27 different optic branches expected in this compound.¹⁷ However, in the calculation of $C_{lattice}$, only three different θ_E 's, each one corresponding to a group of nine optic branches, are taken into consideration.

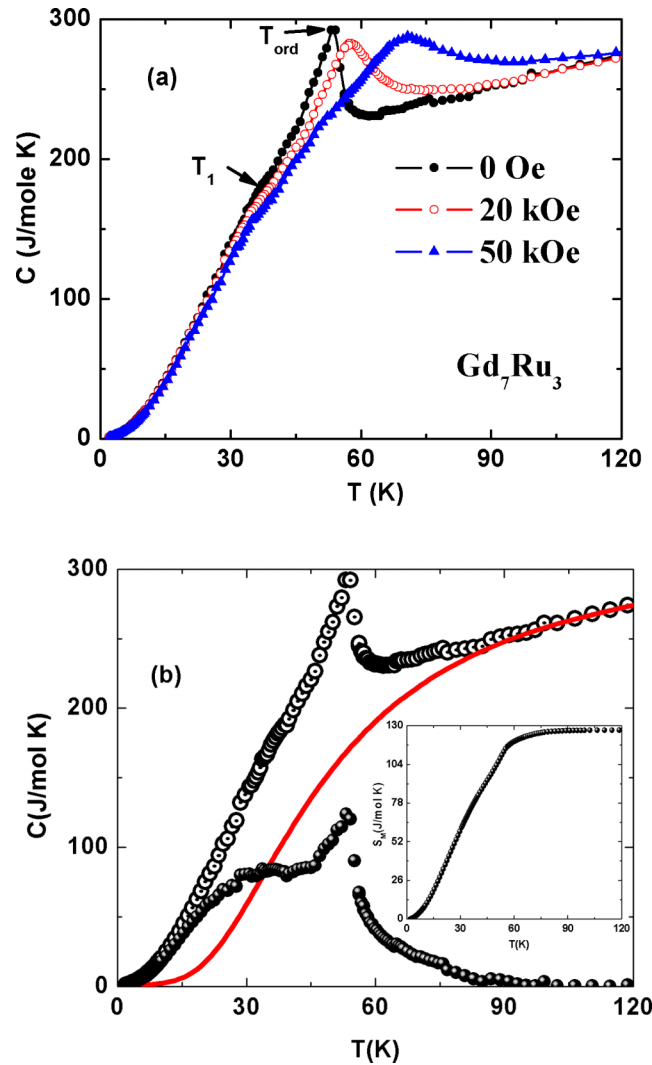


FIG. 4. (a) Temperature dependent heat capacity in applied fields of 0, 20, 50 kOe. The arrows in the figure indicate the ordering temperature (T_{ord}) and the low temperature transition seen at T_1 . (b) Temperature variation of zero field heat capacity. Open circles represent experimental data and solid red line is the calculated nonmagnetic contribution. Filled spheres represent magnetic contribution. The insets show magnetic entropy vs. temperature in zero fields.

Figure 4(b) shows temperature variation of total heat capacity, nonmagnetic and magnetic contribution of the Gd_7Ru_3 compound whereas; inset shows the temperature variation of magnetic entropy of these compounds. The parameters used for calculating the nonmagnetic contribution to the heat capacity are given in table I.

It may be mentioned here that C_{mag} at low temperatures, neither shows $T^{3/2}$ nor T^3 dependence, and hence indicates that low temperature magnetic state in this compound is neither purely

TABLE I. Calculated values of γ (coefficient of electronic specific heat), θ_E 's (Einstein temperatures), θ_D (Debye temperature), α_E 's (anharmonicity coefficients for the optical branches) and α_D 's (anharmonicity coefficients for the acoustic branches) from zero field heat capacity data.

Compound	γ (mJ mol ⁻¹ K ⁻²)	θ_D (K)	θ_{E1} (K)	θ_{E2} (K)	θ_{E3} (K)	α_E (K ⁻¹)	α_D (K ⁻¹)
Gd_7Ru_3	72	120	144	180	209	1.6×10^{-4}	1.7×10^{-4}

ferromagnetic nor antiferromagnetic. It can be seen from the inset of the figure 4(b) that magnetic entropy shows saturation tendency towards the theoretical value $R\ln(2J+1)$ at temperatures well above T_{ord} , which implies that only few levels of the ground state multiplet are involved in the ordering process.²⁶

The MCE of this compound have been determined in terms of $-\Delta S_M$ and ΔT_{ad} using the heat capacity data in 0, 20 and 50 kOe fields using the equations.¹

$$S(T, H) = \int_0^T \left(\frac{C(T, H)}{T} \right) dT$$

$$\Delta S_M(T, H)_{\Delta H} = \int_0^T \left(\frac{C(T, H) - C(T, 0)}{T} \right) dT$$

$$\Delta T_{\text{ad}}(T)_{\Delta H} \cong [T(S)_{H_f} - T(S)_{H_i}]$$

Similarly, based on the M-H isotherms near ordering temperatures, the change in $-\Delta S_M$ of sample was calculated using the integrated Maxwell relation¹

$$\Delta S_M(T_{\text{av}}, H) = \int_{H_i}^{H_f} \left(\frac{\partial M}{\partial T} \right) dH \approx \frac{1}{\Delta T} \int_{H_i}^{H_f} [M(T_{i+1}, H_i) - M(T_i, H_f)] dH$$

Where $T_{\text{av}} = (T_{i+1} + T_i)/2$ means average temperature and $\Delta T = T_{i+1} - T_i$ means temperature difference between two magnetization isotherms measured at T_{i+1} and T_i with the magnetic field H_i to H_f .

The MCE behavior of amorphous Gd_7Ru_3 has been determined in terms of ΔS_M as well as ΔT_{ad} using heat capacity data in field change of 20 and 50 kOe as shown in figure 5(a) & 5(b).¹ It can be seen from figure 5(a) that ΔS_M vs. T plot shows a maximum near T_{ord} , and ΔS_M do not die out even at temperatures well above 120 K. This may be due to the presence of short range magnetic correlations or spin fluctuations in the paramagnetic state.

The maximum isothermal entropy change (ΔS_M^{max}), for $\Delta H = 50$ kOe and 20 kOe, of this compound is $\sim 21 \text{ J mol}^{-1}\text{K}^{-1}$ and $10 \text{ J mol}^{-1}\text{K}^{-1}$ respectively. It is of interest to note that the ΔS_M^{max} values of (Er/Dy) Al_2 compounds, which are promising magnetic refrigerants in the temperature range of 13 to 60 K, varies in the range of 4.5 to $8.0 \text{ J mol}^{-1}\text{K}^{-1}$, for $\Delta H = 50$ kOe.¹ The ΔS_M^{max} of RNi_2 compounds, which have ordering temperature less than 80 K, varies from 3- $8 \text{ J mol}^{-1}\text{K}^{-1}$, for the same field change.²⁷ ΔS_M^{max} of Gd_2PdSi_3 below 40 K is $\sim 4 \text{ J mol}^{-1}\text{K}^{-1}$ (for

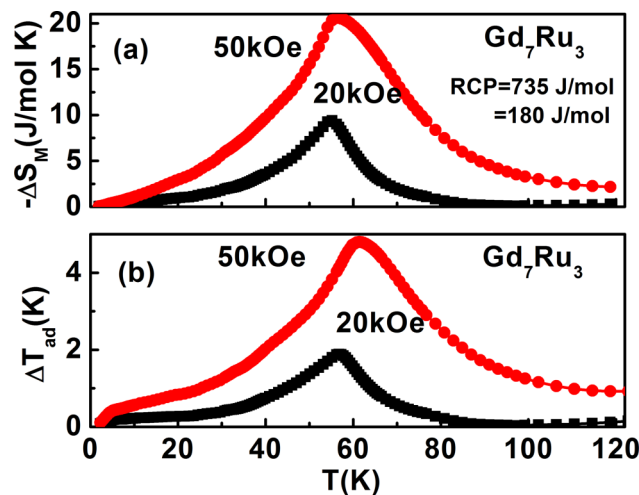


FIG. 5. Temperature dependence of calculated (a) ΔS_M and (b) ΔT_{ad} in applied fields of 20 and 50 kOe.

$\Delta H = 40$ kOe).²⁸ Therefore, the comparison of maximum ΔS_M of present compound with that of the potential magnetic refrigerant materials indicates that, this material is suitable for the refrigeration application below 60 K. In figure 4(b), ΔT_{ad} vs. T plot of this compound is shown at 20 and 50 kOe. The maximum value of ΔT_{ad} (ΔT_{ad}^{max}) at 20 and 50 kOe are ~ 2 and ~ 5 K respectively. The temperature variation of ΔT_{ad} is similar to that of temperature dependence of ΔS_M . Furthermore, the ΔT_{ad}^{max} values HoNiAl are 4 and 8.7 K, for $\Delta H = 20$ and 50 kOe, respectively, whereas for DyNiAl, for the same field changes, these values are found to be 3.5 and 6.8 K, respectively. It may be mentioned here that ΔT_{ad}^{max} value, for $\Delta H = 50$ kOe, of RNi₂ compounds varies in the range of 3.5- 9 K²⁷ whereas for (Er,Dy)Al₂ compounds, for the same field change, this value varies between 7 and 11 K.²⁹ In the material Gd₇Ru₃, large ΔS_M and ΔT_{ad} values persists in a wide temperature range around ordering temperature range. This feature is important to obtain relatively high cooling capacity (RC parameter) and is characteristic of amorphous alloys. Relatively high values of RC parameter, i.e., 180 and 735 J/mol respectively, were obtained for $\Delta H=20$ and 50 kOe. This RC of investigated alloys is comparable to the values determined for Gd₅₅Fe₃₀Al₃₀ and Gd₅₅Fe₂₀Al₂₅.³⁰ However, the value of RC for Gd₇Ru₃ is higher than that of the most classical crystalline magnetic refrigeration materials.³⁰⁻³⁴

CONCLUSIONS

The magneto-thermal properties of amorphous Gd₇Ru₃ have been studied. The magnetocaloric property of this compound is found to be comparable to that of many potential refrigerant materials like (Er/Dy)Al₂, RNi₂, Gd₂PdSi₃ etc. Large RCP, large ΔT_{ad} change, soft magnetic behavior and wide operating temperature range (>120 K) make it an attractive candidate as magnetic refrigerant in low temperature region. The magnetic state of Gd₇Ru₃ has been studied by heat capacity measurements, both, under zero-field as well as in various applied fields.

ACKNOWLEDGMENT

One of the authors (Pramod Kumar) thanks DST, Govt. of India for proving financial support for this work.

- ¹ A.M. Tishin and Y.I. Spichkin, *The Magnetocaloric Effect and its Applications* (IOP, Bristol, 2003); V. Franco, J.S. Blazquez, B. Ingale, and A. Conde, *Annu. Rev. Mater. Res.* **42**, 305 (2012); M. Ghorbani Zavareh, C. Salazar Mejía, A. K. Nayak, Y. Skourski, J. Wosnitza, C. Felser, and M. Nicklas, *Appl. Phys. Lett.* **106**, 071904 (2015); P. Shahi, H. Singh, A. Kumar, K. K. Shukla, A. K. Ghosh, A. K. Yadav, A. K. Nigam, and S. Chatterjee, *AIP Advances* **4**, 097137 (2014); V. Suresh Kumar, Rami Chukka, Zuhuang Chen, Ping Yang, and Lang Chen, *AIP Advances* **3**, 052127 (2013).
- ² K. A. Gschneidner, Jr., V. K. Pecharsky, and A. O. Tsokal, *Rep. Prog. Phys.* **68**, 6 (2005).
- ³ A. Giguère, M. Foldeaki, B. R. Gopal, R. Chahine, T. K. Bose, A. Frydman, and J. A. Barclay, *Phys. Rev. Lett.* **78**, 4494 (1997).
- ⁴ S. Gama, A. A. Coelho, A. de Campos, A. M. G. Carvalho, F. C. G. Gandra, P. J. von Ranke, and N. A. de Oliveira, *Phys. Rev. Lett.* **93**, 237202 (2003).
- ⁵ H. Wada and Y. Tanbe, *Appl. Phys. Lett.* **79**, 3302 (2001); E.J.R. Plaza, V.S.R. de Sousa, M.S. Reis, and P. J. von Ranke, *J. Alloys. Compounds* **505**, 357 (2010).
- ⁶ N. K. Singh, K. G. Suresh, and A.K. Nigam, *Solid State Commun.* **127**, 373 (2003); S. Gupta, R. Rawat, and K. G. Suresh, *Appl. Phys. Lett.* **105**, 012403 (2014).
- ⁷ N. K. Singh, K. G. Suresh, A. K. Nigam, S. K. Malik, A. A. Coelho, and S. Gama, *J. Mag. Mag. Mag.* **317**, 68 (2007); N. K. Singh, P. Kumar, K. G. Suresh, A. K. Nigam, A. A. Coelho, and S. Gama, *J. Phys.: Condensed Matter* **19**, 036213 (2007); N. K. Singh, P. Kumar, K. G. Suresh, and A. K. Nigam, *J. Phys. D: Appl. Phys.* **40**, 1620 (2007); N. K. Singh, P. Kumar, K. G. Suresh, and A. K. Nigam, *J. Appl. Phys.* **105**, 023901 (2009); P. K. Das, A. Bhattacharyya, R. Kulkarni, S. K. Dhar, and A. Thamizhavel, *Phys. Rev. B* **89**, 134418 (2014).
- ⁸ F.-H. Hu, B.-G. Shen, and J.-R. Sun, *Appl. Phys. Lett.* **76**, 3460 (2000).
- ⁹ M. P. Annaorazoy and S. A. Nikitin, *J. Appl. Phys.* **79**, 1689 (1996).
- ¹⁰ W. Chen, W. Zhong, D. L. Hou, R. W. Gao, W. C. Feng, M. G. Zhu, and Y. W. Du, *J. Phys.: Condens. Matter* **14**, 11889 (2002).
- ¹¹ H. Ucar, J. Ipus, V. Franco, M.E. McHenry, and D. Laughlin, *JOM* **64**, 728 (2012).
- ¹² H. Gencer, T. Izgi, V. S. Kolat, N. Bayri, and S. Atalay, *J. Non-Cryst. Solids* **379**, 185 (2013).
- ¹³ V. Franco, J. S. Blazquez, M. Millan, J. M. Borrego, C. F. Conde, and A. Conde, *J. Appl. Phys.* **101**, 09C503 (2007).
- ¹⁴ C. T. Chang, B. L. Shen, and A. Inoue, *Appl. Phys. Lett.* **89**, 051912 (2006).
- ¹⁵ K. H. J. Buschow, H. A. Algra, and R. A. Henskens, *J. Appl. Phys.* **51**, 561 (1980).
- ¹⁶ T. Gao, S. X. Cao, K. Liu, B. J. Kang, L. M. Yu, S. J. Yuan, and J. C. Zhang, *J. Phys.: Conf. Ser.* **150**, 042038 (2009).

- ¹⁷ B. L. Zink and F. Hellman, *Phys. Rev. B* **79**, 235105 (2009).
- ¹⁸ X. Liu and H. V. Lohneysen, *Europhys. Lett.* **33**, 617 (1996).
- ¹⁹ B. L. Zink, R. Pietri, and F. Hellman, *Phys. Rev. Lett.* **96**, 055902 (2006).
- ²⁰ J. L. Feldman, D. J. Singh, I. I. Mazin, D. Mandrus, and B. C. Sales, *Phys. Rev. B* **61**, R9209 (2000); D. M. Liu, Z. L. Zhang, S. L. Zhou, Q. Z. Huang, X. J. Deng, M. Yue, C. X. Liu, F. X. Hu, G. H. Rao, B. G. Shen, J. X. Zhang, and J. W. Lynn, [arXiv:1408.6791](https://arxiv.org/abs/1408.6791).
- ²¹ R. P. Hermann, R. Jin, W. Schweika, F. Grandjean, D. Mandrus, B. C. Sales, and G. J. Long, *Phys. Rev. Lett.* **90**, 135505 (2003).
- ²² V. Keppens, D. Mandrus, B. C. Sales, B. C. Chakoumakos, P. Dai, R. Coldea, M. B. Maple, D. A. Gajewski, E. J. Freeman, and S. Bennington, *Nature (London)* **395**, 876 (1998).
- ²³ P. Javorsky, M. Divis, H. Sugawara, H. Sato, and H. Mutka, *Phys. Rev. B* **65**, 014404 (2001).
- ²⁴ P. Svoboda, P. Javorsky, M. Divis, V. Sechovsky, F. Hona, G. Oomi, and A. A. Menovsky, *Phys. Rev. B* **63**, 212408 (2001).
- ²⁵ J. A. Blanco, D. Gignoux, and D. Schmitt, *Phys. Rev. B* **43**, 13145 (1991).
- ²⁶ J. A. Blanco, D. Gignoux, and D. Schmitt, *Phys. Rev. B* **43**, 13145 (1991); K. Sengupta, K. K. Iyer, and E. V. Sampathkumaran, *Phys. Rev. B* **72**, 054422 (2005).
- ²⁷ P. J. von Ranke, E. P. Nobrega, I. G. de Oliveira, A. M. Gomes, and R. S. Sarthour, *Phys. Rev. B* **63**, 184406 (2001).
- ²⁸ E. V. Sampathkumaran, I. Das, R. Rawat, and S. Majumdar, *Appl. Phys. Lett.* **77**, 418 (2000).
- ²⁹ P. J. von Ranke, V. K. Pecharsky, and K. A. Gschneidner, Jr., *Phys. Rev. B* **58**, 12110 (1998).
- ³⁰ D. Ding, M. B. Tang, and L. Xia, *J. Alloys. Compounds* **581**, 828 (2013).
- ³¹ V. Provenzano, A. J. Shapiro, and R. D. Shull, *Nature* **429**, 853 (2004).
- ³² V. K. Pecharsky and K. A. Gschneidner, *Phys. Rev. Lett.* **78**, 4494 (1997).
- ³³ N. Pierunek, Z. Sniadecki, J. Marcin, I. Skorvanek, and B. Idzikowski, *IEEE Trans. Mag.* **50**, 2506603 (2014).
- ³⁴ S. Gorsse, B. Chevalier, and G. Orveillon, *Appl. Phys. Lett.* **92**, 122501 (2008); E. T. Dias, K. R. Priolkar, O. Cakir, M. Acet, and A. K. Nigam, [arXiv:1503.04276](https://arxiv.org/abs/1503.04276).